JOURNAL OF THERMOPHYSICS AND HEAT TRANSFER
Vol. 18, No. 4, October–December 2004

Strong Magnetic Field Asymptotic Model for Binary Alloyed Semiconductor Crystal Growth

Xianghong Wang* and Nancy Ma†
North Carolina State University, Raleigh, North Carolina 27695

This paper presents an asymptotic model for the unsteady species transport during bulk growth of alloyed semiconductor crystals with a transverse magnetic field. During growth of alloyed semiconductors such as germanium-silicon (GeSi), the solute's concentration is not small, so that density differences in the melt are very large. These compositional variations drive compositionally driven buoyant convection, or solutal convection, in addition to thermally driven buoyant convection. These buoyant convections drive convective transport, which produces nonuniformities in the concentration in both the melt and the crystal. This transient model predicts the melt motion and the distribution of species for a crystal grown in a strong transverse magnetic field.

I. Introduction

MANY optoelectronic devices are produced on wafers sliced from crystals of alloyed photonic semiconductors, such as germanium-silicon (GeSi), and are grown by various processes such as Bridgman crystal growth or directional solidification. Recent rapid advances in optoelectronics have led to a great demand for more and larger crystals with fewer dislocations and other microdefects, and with uniform and controllable compositions in alloyed semiconductor crystals. For the growth of a binary alloyed crystal, the crystal is grown from a mixture of two components, and one component is generally rejected back into the melt. For example, germanium is rejected into the melt along the crystal-melt interface during the growth of GeSi, leading to a large concentration of germanium near the growth interface. Anything that causes this elevated concentration to become nonuniform across the interface leads to compositional variations in the crystal between the center and the periphery, called radial macrosegregation. Density differences caused by both compositional and thermal variations in the melt drive compositionally driven and thermally driven buoyant convection, respectively, which lead to compositional variations both in the melt and in the crystal.

Because molten semiconductors are excellent electrical conductors, an externally applied magnetic field can be used to create a body force that provides an electromagnetic (EM) damping of the melt motion and can be used to control the species transport in order to optimize the compositional distribution during the growth process.[1] If the EM damping is extremely strong, then the melt motion is suppressed and has no effect on the composition in the crystal, and then this diffusion-controlled species transport can produce a laterally and axially uniform composition in the crystal except in the first-grown and last-grown parts of the crystal. To achieve diffusion-controlled species transport, the species transport Péclet number $Pe_m = U_c L/D$ must be small, where U_c is the characteristic velocity for the magnetically damped melt motion and is inversely proportional to the square of the magnetic flux density B_0, while L is the characteristic dimension of the melt and D is the diffusion coefficient for the species in the molten semiconductor. If $Pe_m \ll 1$, then the characteristic ratio of convection to diffusion of the species is small, and the species transport is diffusion controlled. However, because typical values[2] of D are 1 to 2×10^{-8} m^2/s, B_0 must be extremely large for diffusion-controlled species transport so that diffusion-controlled growth is not possible on Earth.[3,4] Therefore, the objective is to identify a magnetic field strength and orientation in order to achieve both lateral and axial compositional uniformity in the crystal. The large number of adjustable crystal growth parameters and the larger number of ways to combine them makes process optimization through trial and error almost impossible and not reproducible so that models that predict the alloy distribution in the crystal are very useful.

During the melt growth of alloyed semiconductor crystals, the application of magnetic fields has shown great promise. For example, Watring and Lehoczky[5] have shown that the radial variation between the maximum and minimum concentrations can be decreased by more than a factor of three with the application of a 5 T magnetic field, arising because the magnetic field retards the sinking of the heavier melt to the center of the ampoule, resulting in less radial segregation. Ramachandran and Watring[6] reported a reduction in the radial segregation in all of their samples that were grown in a magnetic field.

For alloyed semiconductor crystal growth, the density differences caused by compositional variations in the melt are very large. In GeSi, for example, the mole fraction of germanium can vary from 0.95 in the melt, which has not yet received any rejected germanium to 0.99 near the interface, and this compositional difference corresponds to a density difference of nearly 300 kg/m^3. In a frequently used extension of the Boussinesq approximation, the melt density is assumed to vary linearly with both the temperature and mole fraction of either species. In this approximation, the magnitudes of the density difference and of the resultant buoyant convection associated with the temperature variation or with the compositional variation are characterized by $\beta_T(\Delta T)_0$ and $\beta_C C_0$, respectively, where β_T and β_C are the thermal and compositional coefficient of volumetric expansion, while $(\Delta T)_0$ and C_0 are the characteristic radial temperature difference and the initially uniform mole fraction of the species, that is, of silicon in the GeSi melt. For GeSi with $(\Delta T)_0 = 10$ K and $C_0 = 0.05$, the characteristic ratio of the buoyant convection driven by thermal variations to that driven by compositional variations is $\beta_T(\Delta T)_0/\beta_C C_0 = 0.125$. Although the thermally driven buoyant convection is probably not negligible, particularly far from the crystal-melt interface where compositional variations are small, the compositionally driven buoyant convection or soluto-convection is dominant particularly near the interface.

In a previous study,[7] we presented an asymptotic and numerical solution for the dilute species transport during the solidification of a GeSi crystal with a transverse magnetic field. This study only considered pure crystals with very small dopant concentrations so that there was only thermally driven buoyant convection, where the

Received 28 October 2003; accepted for publication 9 June 2004.

*Graduate Research Assistant, Department of Mechanical and Aerospace Engineering, Campus Box 7910, 2601 Stinson Drive.

†Assistant Professor, Department of Mechanical and Aerospace Engineering, Campus Box 7910, 2601 Stinson Drive; nancy_ma@ncsu.edu. Senior Member AIAA.

velocity and temperature were independent of the dopant concentration and known at each time step, and the governing equation for species conservation was a linear equation with known spatially variable coefficients given by an analytical solution for velocity. During growth of alloyed semiconductor crystals, the velocity and mole fraction of either species are intrinsically coupled because the buoyant convection is driven by both thermal and compositional variations in the melt. In the 1970s, Hart[8] presented an asymptotic and numerical solution for the motion of a stratified salt solution with both thermally driven and compositionally driven buoyant convection and without a magnetic field or solidification. In the present paper, we extend these studies[7,8] to treat both thermally driven and compositionally driven buoyant convection during the solidification of a GeSi crystal with a transverse magnetic field. Several crystal growers are currently performing experiments on the solidification of germanium crystals with various amounts of silicon and with magnetic fields.[9,10] We use a two-dimensional model problem in a horizontal container to develop an asymptotic method and to provide physical insight, but the extension to three-dimensional melt motions in actual crystal growth processes would be straightforward.

II. Problem Formulation

We treat the unsteady, two-dimensional species transport of a species in a solidifying, electrically conducting semiconductor melt in a horizontal, rectangular container with thermally insulated top and bottom walls and with an externally applied, uniform, steady vertical (or transverse) magnetic field $B_0\hat{\boldsymbol{y}}$, as shown in Fig. 1. Here, B_0 is the magnetic flux density, while $\hat{\boldsymbol{x}}$, $\hat{\boldsymbol{y}}$, and $\hat{\boldsymbol{z}}$ are the unit vectors for the Cartesian coordinate system. The coordinates and lengths are normalized by half the distance between the top and bottom walls L, and a is the dimensionless length of the container. The constant uniform heat flux q into the right end of the container keeps the semiconductor molten. The heat flux removed at the left end of the container is adjusted so that the crystal-melt interface moves at a constant velocity $U_g = \omega U_c$, where ω is the dimensionless interface velocity. With time t normalized by L/U_c, the dimensionless time to grow the entire crystal is a/ω.

Experiments[5] have shown that magnetic fields can control compositionally driven buoyant convection so that the electromagnetic body force must be comparable to the characteristic gravitational body force associated with compositional variations. Because the electric currents only arise from the melt motions across the magnetic field, the magnetic field can damp the motion but cannot completely suppress it. Therefore, this balance gives a characteristic velocity for the magnetically damped compositionally driven buoyant convection[11]

$$U_c = \frac{\rho_0 g \beta_c C_0}{\sigma B_0^2} \tag{1}$$

where ρ_0 is the melt's density at the solidification temperature T_0, g is gravitational acceleration, and σ is the electrical conductivity of the melt. Thus we can expect the melt motion to decrease roughly as B_0^{-2} as the magnetic field strength is increased.

The electric current in the melt produces an induced magnetic field, which is superimposed on the applied magnetic field produced by the external magnet. The characteristic ratio of the induced to the applied magnetic field strengths is the magnetic Reynolds number $R_m = \mu_p \sigma U_c L$, where μ_p is the magnetic permeability of the melt. For all crystal growth processes, $R_m \ll 1$, and the additional magnetic fields produced by the electric currents in the melt are negligible.

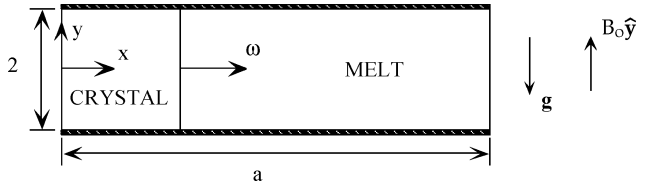

Fig. 1 Two-dimensional model problem with a uniform, steady transverse magnetic field $\boldsymbol{B} = \hat{\boldsymbol{y}}$, and with coordinates normalized by half the distance between the top and bottom walls.

We assume that the temperature differences and compositional variations are sufficiently small so that all of the physical properties of the melt can be considered uniform and constant except for the density in the gravitational body force term of the Navier–Stokes equation. In this Boussinesq-like approximation, the characteristic temperature difference $(\Delta T)_0$ and the characteristic mole fraction difference $(\Delta C)_0$ are assumed to be sufficiently small so that the melt's density is a linear function of temperature and composition, given by

$$\rho = \rho_0\left[1 - \beta_T\left(T^* - T_0\right) - \beta_c\left(C^* - C_0\right)\right] \tag{2}$$

and that $\beta_T(\Delta T)_0 \ll 1$ and $\beta_C(\Delta C)_0 \ll 1$, where T^* is the temperature in the melt and C^* is the mole fraction of one species in the melt.

The equations governing the melt motion, heat transfer, and species transport are

$$N^{-1}\left[\frac{\partial \boldsymbol{v}}{\partial t} + (\boldsymbol{v}\cdot\nabla)\cdot\boldsymbol{v}\right] = -\nabla p + (\gamma T + C - 1)\hat{\boldsymbol{y}} + \boldsymbol{j}\times\hat{\boldsymbol{y}} + Ha^{-2}\nabla^2\boldsymbol{v} \tag{3a}$$

$$\nabla\cdot\boldsymbol{v} = 0 \tag{3b}$$

$$\nabla\cdot\boldsymbol{j} = 0 \tag{3c}$$

$$\boldsymbol{j} = -\nabla\phi + \boldsymbol{v}\times\hat{\boldsymbol{y}} \tag{3d}$$

$$Pe_t\left[\frac{\partial T}{\partial t} + (\boldsymbol{v}\cdot\nabla)T\right] = \nabla^2 T \tag{3e}$$

$$Pe_m\left[\frac{\partial C}{\partial t} + (\boldsymbol{v}\cdot\nabla)C\right] = \nabla^2 C \tag{3f}$$

$$C = \frac{C^*}{C_0} \tag{3g}$$

$$T = \frac{T^* - T_0}{(\Delta T)_0} \tag{3h}$$

$$\gamma = \frac{\beta_T(\Delta T)_0}{\beta_c C_0} \tag{3i}$$

where p is the deviation of the pressure from the hydrostatic pressure for the uniform density ρ_0 normalized by $\sigma U_c B_0^2 L$, ϕ is the electric current potential normalized by $U_c B_0 L$, T is the deviation of the dimensional melt's temperature from the solidification temperature normalized by $(\Delta T)_0$, C is the mole fraction normalized by its initially uniform value C_0, and $\boldsymbol{v} = u\hat{\boldsymbol{x}} + v\hat{\boldsymbol{y}}$ is the dimensionless velocity. Here, u and v are the horizontal and vertical velocities, respectively, normalized by U_c. The characteristic ratio of the EM body force to the inertial force is the interaction parameter $N = \sigma^2 B_0^4 L/\rho_0^2 g\beta_C C_0$. The square root of the characteristic ratio of the EM body force to the viscous force is the Hartmann number $Ha = B_0 L(\sigma/\mu)^{1/2}$. Equations (3b) and (3c) are continuity of mass and of electric current, respectively, while Eq. (3d) is Ohm's law. In conservation of energy given by Eq. (3d), the characteristic ratio of the convective to conductive heat transfer is the thermal Péclet number $Pe_t = \rho_0^2 g\beta_c C_0 c_p L/k\sigma B_0^2$, where c_p and k are the specific heat and the thermal conductivity of the melt, respectively. Equation (3f) is conservation of species for the solute in the molten semiconductor. During the growth of a GeSi crystal for $C_0 = 0.05$ in a 2 T magnetic field with $(\Delta T)_0 = 10$ K, $U_c = 0.000421$ m/s, $N = 25{,}889$, $Ha = 793.33$, $Pe_t = 0.2528$, $Pe_m = 158.02$, and $\gamma = 0.08$.

In our two-dimensional model problem, nothing varies in the z direction, and there can be a uniform electric field in the z direction E_z. In any actual horizontal Bridgman process, there are electrically insulating walls at, say, $z = \pm d$, which block any electric current in

the z direction. For the present recirculating flow, $E_z = 0$ for zero net electric current. The electric current density normalized by $\sigma U_c B_0$ and Ohm's law give $\boldsymbol{j} = u\hat{\boldsymbol{z}}$.

For a sufficiently strong magnetic field, Pe_t is small, so that the convective heat-transfer terms in Eq. (3e) are negligible. Ma and Walker[12] found that the error caused by neglect of convective heat transfer is less than 4% for $Pe_t \leq 15.0$, so that convective heat transfer is certainly negligible for our present process with $Pe_t = 0.2528$. With negligible convective heat transfer, the crystal-melt interface is planar as shown in Fig. 1. In general, $U_g < U_c$, so that the heat released by the cooling melt is negligible compared to the conductive heat transfer.[13,14] Therefore, the heat flux through the melt is uniform and constant, and the deviation of the melt's temperature from T_0, normalized by $Lq/k = (\Delta T)_0$, is

$$T = x - \omega t \tag{4}$$

In the Navier–Stokes equation, inertial terms are negligible for a sufficiently strong magnetic field. In a recent study, Ma and Walker[12] found that the error caused by the neglect of inertial effects is only 2.7% for $N = 16.59$ and is totally negligible for $N \geq 648.1$, so that inertial effects are certainly negligible for our present process with $N = 25{,}889$. In an asymptotic solution for $Ha \gg 1$ for our inertialess melt motion, the melt is divided into an inviscid core, Hartmann layers with $\mathcal{O}(Ha^{-1})$ thickness, and parallel layers with $\mathcal{O}(Ha^{-1/2})$ thickness. Here, $\xi = [2x - (a + \omega t)]/(a - \omega t)$ is our rescaled axial coordinate so that $-1 \leq \xi \leq +1$ for all time. The Hartmann layers lie adjacent to the top and bottom walls, while the parallel layers lie adjacent to the crystal-melt interface and the right end of the container. The Hartmann layers carry an $\mathcal{O}(Ha^{-1})$ flow that has a simple, local, exponential structure, which matches any core or parallel velocity, and which satisfies the no-slip conditions along the crystal-melt interface or container wall. Although the Hartmann layers represent an extremely small fraction of the melt's volume and flow rate, the parallel layers occupy a significant fraction of the melt and carry an $\mathcal{O}(Ha^{1/2})$ velocity. Therefore, a formal asymptotic analysis for $Ha \gg 1$ is not appropriate, but the numerical solution of the inertialess Navier–Stokes equation with all of the viscous terms is not necessary. Thus, we use a hybrid solution, which does not assume that the parallel layer's thickness is small. This hybrid solution neglects the $\mathcal{O}(Ha^{-1})$ volume flux deficiency in the Hartmann layers and the $\mathcal{O}(Ha^{-1})$ perturbation in the parallel layers.

We discard the viscous terms $Ha^{-2}\partial^2 \boldsymbol{v}/\partial y^2$ in the Navier–Stokes equation, and we relax the no-slip conditions at both $y = \pm 1$ because they are satisfied by the Hartmann layers, which are not part of the hybrid solution. We apply the boundary conditions $v = 0$ along $y = \pm 1$, and we apply the no-slip and no-penetration conditions along $\xi = \pm 1$. Because the core carries an $\mathcal{O}(1)$ flow, the flow circuit must be completed through two high-velocity parallel layers with $u = \mathcal{O}(1)$ and $v = \mathcal{O}(Ha^{1/2})$ inside these layers at $\xi = \pm 1$. At the beginning of growth with $a = 1$, the concentration in the melt is uniform, and the melt motion is driven entirely by thermally driven buoyant convection as shown in Fig. 2 for $B_0 = 2$ T and $C_0 = 0.05$. In Fig. 2, the maximum value of the streamfunction is 0.0410, where the streamfunction is

$$u = \frac{\partial \psi}{\partial y} \tag{5a}$$

$$v = -\frac{2}{a - \omega t}\frac{\partial \psi}{\partial \xi} \tag{5b}$$

For the species transport, along each of the other surfaces there cannot be diffusion of species into the impermeable container, so that $\nabla C \cdot \hat{\boldsymbol{n}} = 0$ along each of the surfaces of the container, where $\hat{\boldsymbol{n}}$ is the unit normal vector. Along the crystal-melt interface,

$$\frac{\partial C}{\partial \xi} = -\frac{(a - \omega t)}{2} Pe_g (1 - k_s) C \qquad \text{at} \qquad \xi = -1 \tag{6}$$

where $Pe_g = U_g L/D = \omega Pe_m$ is the growth Péclet number and k_s is the segregation coefficient. The segregation coefficient for silicon in a germanium melt is greater the unity, and so germanium is rejected along the crystal-melt interface. A curve fit based on the binary phase diagram for germanium-silicon presented by Olesinski and Abbaschian[15] gives a relationship for $k_s(C^*)$:

$$k_s(C^*) = 4.2 - 8.7C^* + 6.0C^{*2} + 3.3C^{*3} - 3.8C^{*4} \tag{7}$$

Assuming that there is no diffusion of species in the solid crystal $C_s(x, y)$, normalized by the initial uniform concentration in the melt, is given by

$$C_s(x, y) = k_s C(\xi = -1, y, t = x/\omega) \tag{8}$$

We use a Chebyshev spectral collocation method for the spatial derivatives in the inertialess form of the Navier–Stokes equation (3a) with T given by Eq. (4) and for the spatial derivatives in species transport equation (3f) with Gauss–Lobatto collocation points in ξ and y. For the time derivative in Eq. (3f), we use a second-order-implicit time-integration scheme. We integrate from $t = 0$ to a t that is slightly less than a/ω. We use a large enough number of collocation points in each direction for both the streamfunction and concentration at each time step so that the velocity and concentration gradients are resolved. We systematically increased the numbers of collocations points in the ξ and y directions. Once we reached 31 collocation points in ξ and 31 collocation points in y, there was no change in the maximum and minimum values of ψ and C. For example, these values were exactly the same when we used 101 collocation points in ξ and 101 collocation points in y. We also used a large enough number of time steps such that the results do not change by increasing the number of time steps. For example, when we doubled the number of time steps from 12,800 to 25,600 the minimum value of the concentration changed by only 0.11%, and the maximum value of the streamfunction changed by 0.53%.

At the beginning of crystal growth, the concentration of silicon, normalized with the initial uniform concentration, is $C(\xi, y, t = 0) = 1$. Thus the amount of silicon initially in the melt is obtained by integrating across the ampoule's volume giving a total dimensionless silicon concentration equal to $2a$. We verify that the sum of the total silicon in the melt and in the crystal is equal to $2a$ at each time step.

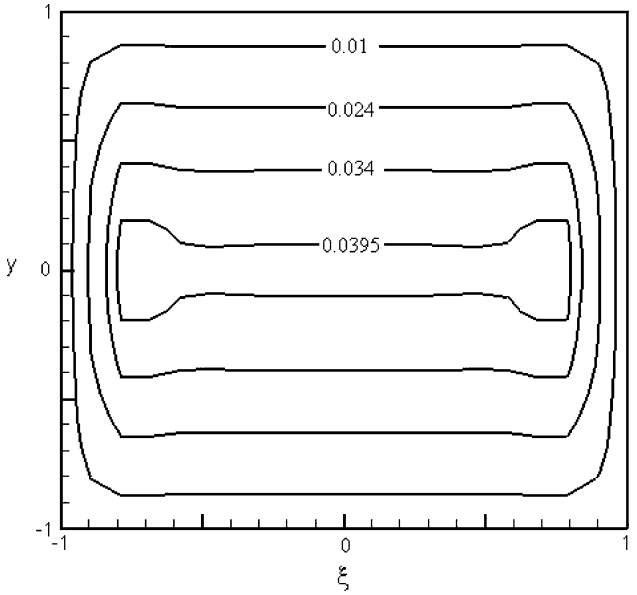

Fig. 2 Streamlines at the beginning of growth for $a = 1$, $B_0 = 2$ T, and $C_0 = 0.05$.

III. Results

We present results for the growth of a germanium-silicon crystal for $a = 1$, $C_0 = 0.05$, $B_0 = 2$ T, and $U_g = 1$ μm/s. For this case $U_c = 0.000421$ m/s, the dimensionless parameters are $\omega = 0.00237$,

$Ha = 793.33$, $Pe_m = 158.02$, and the dimensionless time to grow the crystal is 421.38.

Just before solidification begins at $t = 0$, the melt motion is driven entirely by thermally driven buoyant convection, and the maximum value of the streamfunction is $\psi_{\max} = 0.04102$, as reflected in Fig. 2. The uniform temperature gradient causes the streamlines to be symmetric about $\xi = 0$ and $y = 0$. With a transverse magnetic field, the $\mathcal{O}(Ha^{1/2})$ hotter fluid near $\xi = +1$ quickly flows vertically upward and flows to the left for $y > 0$. When the fluid reaches the colder end of the container near the crystal-melt interface, the $\mathcal{O}(Ha^{1/2})$ colder fluid quickly flows vertically downward, and either solidifies or turns and flows to the right for $y < 0$.

The solidification of the crystal generates a silicon-depleted region along the solidification interface because $k_s > 1$. The heavier silicon-depleted melt drives vertically downward compositionally driven buoyant convection, which is in the same direction of the thermally driven buoyant convection, and therefore increases the value of the streamfunction. Figures 3a and 3b present the contours of the concentration and streamfunction in the melt, respectively, for $t = 4.21$ when 1% of the crystal has solidified. The increase in the flow as a result of the compositionally driven buoyant convection is reflected in the increase in the maximum value of the streamfunction $\psi_{\max} = 0.08935$, which is more than double the value at $t = 0$ before solidification begins. In Fig. 3a, the minimum value of the concentration in the melt is $C_{\min} = 0.7499$, whereas a region of the melt far away from the crystal-melt interface remains at the initial concentration level because the silicon-depleted melt has not had time to convect or diffuse into this region. The minimum value of the concentration is always at the stagnation point in the lower-left corner at $\xi = -1$ and $y = -1$ because the crystal absorbs the silicon and the high-velocity flow adjacent to the crystal-melt interface convects the silicon-depleted melt downward to this region. The $\mathcal{O}(Ha^{1/2})$ downward velocity adjacent to the crystal-melt interface immediately sweeps the silicon-depleted melt creating the long vertical sections of the $C = 0.96$ and 0.92 contours near the crystal-melt interface. The large concentration gradient near the interface has caused the center of rotation of the melt to be greatly shifted towards the interface.

Figures 4a and 4b present the contours of the concentration and streamfunction in the melt, respectively, at $t = 294.98$ when 70% of the crystal has grown. The small amount of silicon remaining in the melt has caused a decrease in the compositionally driven buoyant convection so that the maximum value of the streamfunction has decreased to $\psi_{\max} = 0.04256$. Here, the minimum and maximum

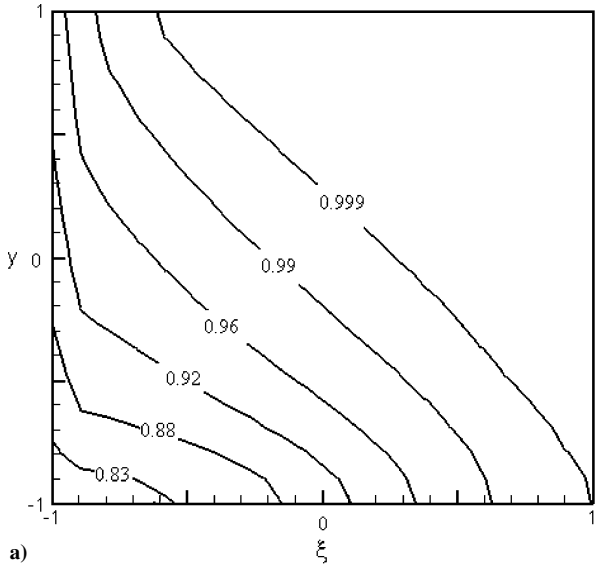

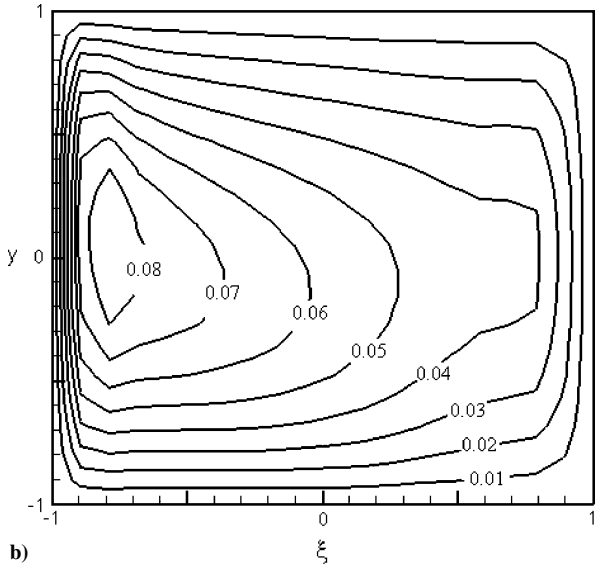

Fig. 3 Contours of the concentration and of the streamfunction in the melt at $t = 4.21$ for $a = 1$, $B_0 = 2$ T, and $C_0 = 0.05$: a) $C(\xi, y, t = 4.21)$ and b) $\psi(\xi, y, t = 4.21)$.

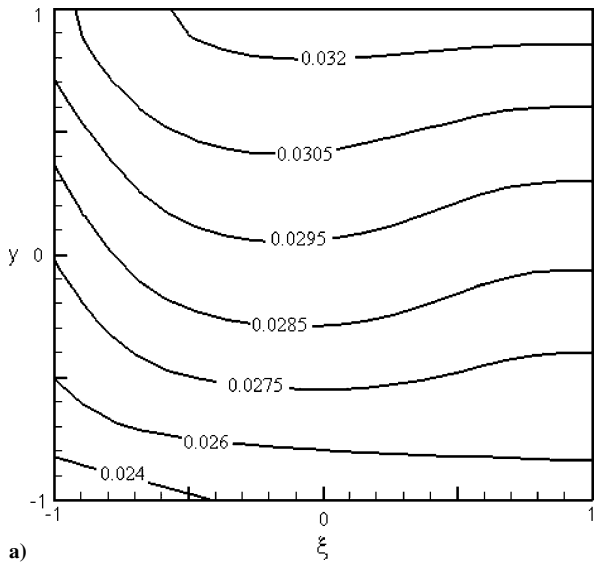

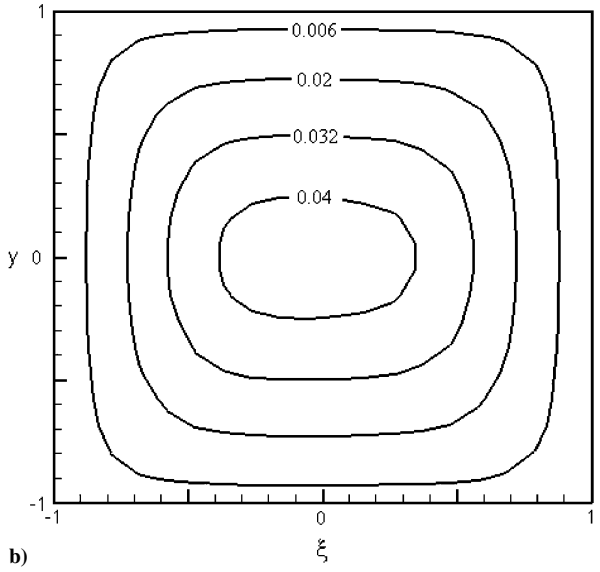

Fig. 4 Contours of the concentration and of the streamfunction in the melt at $t = 294.98$ for $a = 1$, $B_0 = 2$ T, and $C_0 = 0.05$: a) $C(\xi, y, t = 294.98)$ and b) $\psi(\xi, y, t = 294.98)$.

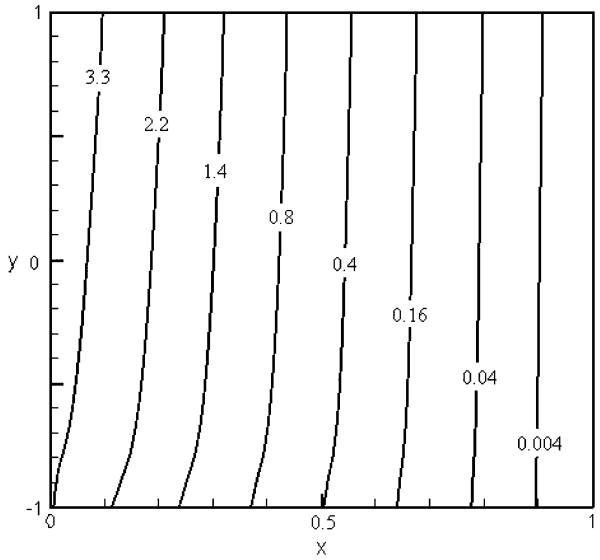

Fig. 5 Contours of the concentration in the crystal for $a = 1$, $B_0 = 2$ T, and $C_0 = 0.05$.

values of the concentration are 0.02236 and 0.03293, respectively. The silicon-depleted melt has convected or diffused everywhere in the melt. The $\mathcal{O}(Ha^{1/2})$ velocities adjacent to the crystal-melt interface and the right end of the container have provided a strong convection of the silicon-depleted melt so that there is significant lateral segregation in the melt. However, because the segregation coefficient is large the difference between the maximum and minimum concentrations in the melt is only $\Delta C = 0.0106$, and the concentration gradient is relatively small compared with earlier stages of growth. Furthermore, this decrease in the contribution of the compositionally driven buoyant convection has caused the streamlines in Fig. 4b to become more symmetric about $\xi = 0$ and $y = 0$.

The contours of the crystal's concentration are shown in Fig. 5. Near the beginning of growth, the transverse magnetic field convects the silicon-depleted melt vertically downward adjacent to the crystal-melt interface so that there the lateral segregation is more severe for the first-grown section of the crystal. As time passes and crystal growth progresses, the lateral segregation decreases for two reasons. First, the melt becomes more mixed, so that the difference between the maximum and minimum values of the concentration decreases. Second, the crystal continually absorbs a significant amount of silicon so that the amount of silicon left in the melt is small. The combination of these two factors causes both the value of the concentration in the melt and the variation of the concentration along the crystal-melt interface to decrease as crystal growth progresses, as reflected in Fig. 5. The decrease in the crystal's axial concentration is also reflected in Fig. 5. Much of the silicon is solidified in the crystal at the beginning of the process, so that as time progresses the silicon-depleted melt continues to become further depleted until the crystal is fully grown at $t = 421.38$. This high level of absorption of silicon into the crystal basically leaves a totally depleted melt by the end of growth so the crystal's concentration is $C_s = 0$ at $x = 1$. Unfortunately, there is severe axial segregation as a result of the large value of the segregation coefficient.

IV. Conclusions

We have developed a method that we can use to predict solutal convection during the melt growth of binary alloyed semiconductor crystals in a strong magnetic field. During the present process, the combination of the large velocity in the melt adjacent to the crystal-melt interface and the large segregation coefficient creates a crystal with a low level of lateral segregation or relatively good lateral homogeneity. However, the extremely high value of k_s causes the crystal to solidify with extremely elevated concentration in the first-grown part of the crystal and leaves the last-grown part of the crystal with virtually no silicon. These results have not been experimentally validated because we treat a model problem in order to develop a method and provide physical insight.

Acknowledgments

This research was supported by NASA under Grant NAG8-1817 and by the U. S. Air Force Office of Scientific Research under Grant FA9550-04-1-0249. The calculations were performed on the Cray X1 provided by the U.S. Department of Defense High Performance Computing Modernization Program under Grant AFSNH2487 and on the IBM P690 provided by the National Science Computational Alliance under Grant DMR030015.

References

[1]Chedzey, H. A., and Hurle, D. T. J., "Avoidance of Growth-Striae in Semiconductor and Metal Crystals Grown by Zone-Melting Techniques," *Nature*, Vol. 210, May 1966, pp. 933–934.

[2]Khine, Y. Y., Banish, R. M., and Alexander, J. I. D., "Convective Contamination in Self-Diffusivity Experiments with an Applied Magnetic Field," *Journal of Crystal Growth*, Vol. 250, No. 1/2, 2003, pp. 274–278.

[3]Alexander, J. I. D., Garandet, J. P., Favier, J. J., and Lizée, A., "g-Jitter Effects on Segregation During Directional Solidification of Tin-Bismuth in the MEPHISTO Furnace Facility," *Journal of Crystal Growth*, Vol. 178, No. 4, 1997, pp. 657–661.

[4]Ma, N., and Walker, J. S., "Magnetic Damping of Buoyant Convection During Semiconductor Crystal Growth in Microgravity. Continuous Random *g*-jitters," *Physics of Fluids*, Vol. 8, No. 4, 1996, pp. 944–953.

[5]Watring, D. A., and Lehoczky, S. L., "Magneto-Hydrodynamic Damping of Convection During Vertical Bridgman-Stockbarger Growth of HgCdTe," *Journal of Crystal Growth*, Vol. 167, No. 3/4, 1996, pp. 478–487.

[6]Ramachandran, N., and Watring, D. A., "Convection Damping by an Axial Magnetic Field During Growth of HgCdTe by Vertical Bridgman Method—Thermal Effects," AIAA, Paper 97-0450, Jan. 1997.

[7]Hirtz, J. M., and Ma, N., "Dopant Transport During Semiconductor Crystal Growth. Axial Versus Transverse Magnetic Fields," *Journal of Crystal Growth*, Vol. 210, No. 4, 2000, pp. 554–572.

[8]Hart, J. E., "On Sideways Diffusive Instability," *Journal of Fluid Mechanics*, Vol. 49, Sept. 1971, pp. 279–288.

[9]Garandet, J. P., and Alboussière, T., "Bridgman Growth: Modelling and Experiments," *The Role of Magnetic Fields in Crystal Growth*, Progress in Crystal Growth and Characterization of Materials, Vol. 38, edited by K. W. Benz, Elsevier, UK, 1999, pp. 73–132.

[10]Matthiesen, D. H., Wargo, M. J., Motakef, S., Carlson, D. J., Nakos, J. S., and Witt, A. F, "Dopant Segregation During Vertical Bridgman-Stockbarger Growth with Melt Stabilization by Strong Axial Magnetic Fields," *Journal of Crystal Growth*, Vol. 85, No. 3, 1987, pp. 557–560.

[11]Ma, N., "Solutal Convection During Growth of Alloyed Semiconductor Crystals in a Magnetic Field," *Journal of Thermophysics and Heat Transfer*, Vol. 17, No. 1, 2003, pp. 77–81.

[12]Ma, N., and Walker, J. S., "Inertia and Thermal Convection During Crystal Growth with a Magnetic Field," *Journal of Thermophysics and Heat Transfer*, Vol. 15, No. 1, 2001, pp. 50–54.

[13]Ma, N., and Walker, J. S., "Dopant Transport During Semiconductor Crystal Growth with Magnetically Damped Buoyant Convection," *Journal of Crystal Growth*, Vol. 172, No. 1/2, 1997, pp. 124–135.

[14]Ma, N., and Walker, J. S., "Validation of Strong Magnetic Field Asymptotic Models for Dopant Transport in Semiconductor Crystal Growth," *Journal of Crystal Growth*, Vol. 180, No. 3/4, 1997, pp. 401–409.

[15]Olesinski, R. W., and Abbaschian, G. J., "The Ge-Si (Germanium-Silicon) System," *Bulletin of Binary Phase Diagrams*, Vol. 5, No. 2, 1984, pp. 180–183.